Influence of Groundwater Management on Land Subsidence in Deltas

A Case Study of Jakarta (Indonesia)

Mahmoud Bakr

Abstract This paper examines effects of groundwater management on land subsidence taking into consideration visco-plastic creep and delayed compaction. The method used in this paper decomposes total strain into a direct elastic contribution and a transient viscous contribution. It is applied to a conceptual model that is partially based on real data of geology, land subsidence measurements, and hydrogeology of northern Jakarta, Indonesia. The developed model is conditioned on land subsidence measurements (from 1974 to 2010) using the Maximum a Posteriori method. The calibrated model is used to evaluate effects of four groundwater management scenarios (from 2010 to 2100) on land subsidence. Maintaining piezometric heads at their values of 2010 has not stopped land subsidence while continuous drawdown has led to larger amount of land subsidence. Furthermore, although piezometric heads recovery decreases effective stresses along the subsurface profile, land subsidence continued (at a lower rate) over time due to creep and slow dissipation of excess pore water pressure. The paper also showed that contribution of creep compaction to total land subsidence could be significant. In addition, coupled processes of consolidation and creep compaction leads to a favorable condition where slow dissipation of excess pore water pressure reduces contribution of the creep compaction to total land subsidence at early times at which degrees of consolidation are small and creep rate is large.

Keywords Land subsidence · Groundwater management · Secondary compaction · Soft soils · Jakarta Indonesia · Deltaic environments

M. Bakr (✉)
Computational Modeling and Simulation of Hydro-Systems, National Water Research Center, Fum Ismailiya Canal, P.O. Box 74, Shobra El-Kheima 13411, Cairo, Egypt
e-mail: mahmoud.bakr@nwrc-egypt.org; mahmoud.bakr@gmail.com

M. Bakr
Unit of Soil and Groundwater Systems, Deltares, Delta Research Institute,
P.O. Box 85467, 3508, AL, Utrecht, The Netherlands

1 Introduction

Land subsidence is the lowering of the land surface due to changes that take place underground. It contributes significantly to flood hazards and limits sustainable development of many areas around the world. This is especially the case in low-lying regions such as deltas which accommodate a significant percentage of the human population. Sea-level rise, decreased accretion of fluvial sediment resulting from upstream siltation, urbanization, and land subsidence are all contributing risk factors that increase vulnerability of deltas to riverine and/or coastal flooding (e.g., Tang et al. (1992), Ericson et al. (2006), Gu et al. (2011), Burkett et al. (2002), and Green et al. (2011)). Causes of land subsidence include both natural and anthropogenic causes. Among the most common human-induced factors for land subsidence, is groundwater extraction. In these cases, groundwater flow and land subsidence are coupled processes, especially in basins with extensive spatial extent of soft soils (e.g. clay). The literature contains a large number of useful studies on subsidence as related to fluids (water and oil) and gas extraction from the subsurface (e.g., Helm (1975, 1976), Holzer (1981), Wilson and Gorelick (1996), Zhang et al. (2007), Onta and Gupta (1995), Huang and Shu (2012), and Calderhead et al. (2012)). Galloway and Burbey (2011) present an excellent overview of subsidence research and applications pertaining to aquifer-system compaction that accompanies the extraction of groundwater.

In hydrogeological settings composed of unconsolidated alluvial or basin-fill aquifer systems comprising aquifers and aquitards, aquifer-system compaction causes significant land subsidence. Aquitards are saturated, permeable geologic unit which can only transmit small quantities of water, and they maintain critical controls on groundwater flow systems (Tóth 1995). They can cause very long response times to changes in groundwater flow. One of the primary works addressing analysis of aquifer-system compaction is Jacob (1940). This was based on conventional groundwater flow theory and the pioneering work of Terzaghi (1925) of the principle of effective stress. Jacob (1940), using Theis equation (Theis 1935), derived the differential equation that describes the flow of groundwater in an elastic confined aquifer. Meinzer (1928) presented evidence for compressibility and elasticity derived from laboratory tests and field investigations.

Soft soils that may compose aquitards are extremely complex natural materials where creep is one of its typical properties. The creep deformation (also known as secondary strain) of soils is a secondary consolidation process that leads to a reduction in void ratio at constant effective stress, and consequently, to the development of an apparent pre-consolidation pressure (Den Haan 1994). In the literature, one can find many documented examples of in-situ creep behavior including the uneven settlement of the tower of Pisa in Italy (Vermeer et al. 2002). Buisman (1936) was probably the first to propose a creep law for soft soils to justify unexplained consolidation behavior for clay and peat soils when using the classical consolidation theory by Terzaghi (1925). In his analysis, he considered a primary stage of consolidation and a second stage of secondary consolidation (creep). The two stages were assumed mutually independent and successive. Later, Taylor (1942) reported that, due to secondary compression, there is a family of stress-strain curves rather than a single curve describing the relationship between stress and strain. Each of these curves, called "time lines" (i.e. isochrones), corresponds to a different duration of the applied load in a standard oedometer test. One of the characteristics of the time lines is that each could have a different value of the pre-consolidation pressure. (Bjerrum) confirmed the observations of Taylor, and related the apparent pre-consolidation and the over-consolidation ratio of virgin clays to soil aging. Bjerrum introduced the terms "instant" and "delayed" compaction to describe the

behavior of the soil skeleton in the absence of the pore pressure dissipation effect. The former is to describe strains occurring simultaneously with the increase of effective stresses and the latter represents strains under constant effective stresses. Garlanger (1972) has modeled the characteristics of Bjerrums concept in terms of the well-known recompression, compression, and secondary compression indices. The Dutch Standards Institution (NNI 1991) has adopted a similar concept which is also followed and explained in the next section. This method is based on the work of Den Haan (1994) and is hereafter referred to as "NEN-Bjerrum". The work on secondary compression was also continued by several researchers including, for example, Borja and Kavaznjian (1985), and Mesri and Vardhanabhuti (2005).

The NEN-Bjerrum method (NNI 1991) is used here to calculate direct and visco-plastic compactions due to change in effective stresses as a result of groundwater abstraction. This paper, for the first time in the literature (up to the knowledge of the author), addresses effects of groundwater management on land subsidence taking into consideration creep compaction. The model is applied to a case study that is based on conceptual information about the subsurface as well as piezometric head data at Daan Mogot (DNMG) area located in the north-western part of Jakarta (Deltares et al. 2011). A time series of land subsidence at the studied location is used to condition the geo-mechanical parameters of the NEN-Bjerrum method. In this analysis, the year 1965 is used as a reference year with no land subsidence due to very limited groundwater abstraction. The model developed is used to forecast land subsidence till 2100 as a result of several groundwater management schemes which are based on trend of groundwater piezometric head data available. Moreover, influences of creep compactions and consolidation processes on forecasted total land subsidence are investigated. The model described here is implemented in MATLAB (2011). It uses schematized subsurface lithology as a sequence of layers using their tops and bottoms. All of the NEN-Bjerrum parameters and piezometeric heads time series for each of the lithological layers should also be defined. The model calculates the total, pore water pressure, and effective stresses time series according to unit weights of soil lithology, piezometeric heads time series, and geometry of the layers.

2 Methodology

Compaction models should include conservation and constitutive equations for both the fluid and solid phase. The two phases are coupled through the state of stress. In soil mechanics, it is common to use Terzaghis equation to calculate effective stresses,

$$\sigma = \sigma^T - u \tag{1}$$

where u is the pore water pressure; and σ^T and σ are the total and effective stresses, respectively. So often, this equation is combined with a compressibility modulus of soil to calculate compaction (e.g., Leake and Galloway (2007)). Here, calculated effective stresses are used to calculate subsurface compaction using the NEN-Bjerrum method.

2.1 The NEN-Bjerrum Method

As mentioned in the introduction section that Bjerrum was the first to notice that creep rate depends on both over-consolidation ratio and age; hence, his name is attached to this model. The NEN-Bjerrum method decomposes total strain into two components; namely, a direct elastic contribution (ε_d) and a transient viscous contribution (ε_{vp}) where all inelastic compression is assumed to result from visco-plastic creep. The method assumes that creep

rate will reduce with increasing over-consolidation and that over-consolidation will grow by unloading and by ageing. Den Haan (1994) has developed the full mathematical formulation. The elastic component is determined by the recompression (unloading) ratio (RR) such that,

$$\varepsilon_{d,t} = RR \, \log\left(\frac{\sigma_t}{\sigma_0}\right) \tag{2}$$

Here, $\varepsilon_{d,t}$ is direct strain at time t; σ_t is effective stress at time σ_t; σ_0 is initial stress at the beginning of simulation.

The transient visco-plastic (creep) component at time t is derived from the viscous creep rate (which depends on the effective stress value at time t, the already reached creep strain at that time and the current over-consolidation ratio as related to the pre-consolidation stress at initial time; (Den Haan 1994). The creep component is mathematically defined as

$$\varepsilon_{vp,t} = C_\alpha \, \log\left(1 + \int_0^t \left(\frac{\sigma_t}{\sigma_{p,0}}\right)^{\frac{CR-RR}{C_\alpha}} \frac{d\tau}{\tau_0}\right) \tag{3}$$

where τ_0 is the creep rate reference time which can be interpreted as the ratio between 1 *day* and the unit of time used in the calculation $[T]$; CR is the compression ratio $[-]$; C_α is the coefficient of secondary compression $[-]$; $\sigma_{p,0}$ is the initial pre-consolidation pressure $[FL^{-2}]$; and $\varepsilon_{vp,t}$ is the visco-plastic compaction at time t $[-]$.

Here, it should be noted that the effective stress ($\sigma_t[FL^{-2}]$) is function of time. Consequently, the integration in Eq. 3 is evaluated numerically. If C_α approaches zero, the creep component in the visco-plastic compaction can be ignored, and the well-known equations of compression and re-compression indices are used instead. In this case, the idealized drained NEN-Bjerrum behavior considers three different cases. The first case occurs when the vertical effective stress at time t (σ_t) is smaller than the pre-consolidation pressure ($\sigma_{p,t}$), then the primary strain contribution can be calculated using

$$\varepsilon_{pr,t} = RR \, \log\left(\frac{\sigma_t}{\sigma_{t-1}}\right), \qquad \sigma_{t-1} < \sigma_t < \sigma_{p,t} \tag{4}$$

The second case in this method is encountered when the vertical effective stress at time t (σ_t) is larger than the pre-consolidation pressure at time t ($\sigma_{p,t}$). In this case, the primary strain contribution according to the idealized behavior can be calculated using the following equation

$$\varepsilon_{pr,t} = RR \, \log\left(\frac{\sigma_{p,t}}{\sigma_{t-1}}\right) + CR \, \log\left(\frac{\sigma_t}{\sigma_{p,t}}\right), \qquad \sigma_{t-1} < \sigma_{p,t} < \sigma_t \tag{5}$$

In Eqs. 4 and 5, $\varepsilon_{pr,t}$ is the primary strain at time t $[-]$.

The third case in this formulation occurs when the vertical effective stress at time step t (σ_t) is smaller than vertical effective stress at initial time (σ_0) which is smaller than the pre-consolidation pressure ($\sigma_{p,t}$); in that case, only swelling takes place and is given by Eq. 2. It should be noted that compression and reloading/swelling ratios are related to compression (C_c) and reloading/swelling (C_r) indices, respectively, as given in Eqs. 6 and 7.

$$CR = \frac{C_c}{1 + e_0} \tag{6}$$

$$RR = \frac{C_r}{1 + e_0} \tag{7}$$

Here, e_0 is initial void ratio $[-]$.

The NEN-Bjerrum method, finally, uses the linear strain model to calculate settlements, such that

$$\Delta b_t = -\varepsilon_t b_0 \tag{8}$$

where Δb_t is settlement at time $t[L]$; ε_t is strain at time t; and b_0 is initial layer thickness $[L]$.

2.2 Consolidation of Multiple Layers

The general one-dimensional vertical consolidation theory by Terzaghi (1925) gives degree of consolidation ($U\ [-]$) as

$$U(t) = 1 - \frac{8}{\pi^2} \sum_{i=1}^{\infty} \left[\frac{1}{(2i-1)^2} \exp\left(-(2i-1)^2 \frac{\pi^2 c_v t}{4d^2} \right) \right] \tag{9}$$

where c_v is consolidation coefficient $[L^2/T]$; d is drainage length $[L]$; i is a counter for term number in the series used to calculate degree of consolidation, and t is consolidation time $[T]$. This equation assumes homogeneous soil and one side drainage. This means that half of the drainage length "d" in Eq. 9 will be used in case of drainage at both sides. To be able to consider consolidation of multiple homogeneous layers of soil between drained layers, equivalent consolidation coefficient is calculated using

$$\frac{\sum_{j=1}^{n} b_j}{\sqrt{\widetilde{c_v}}} = \sum_{j=1}^{n} \frac{b_j}{\sqrt{c_{v,j}}} \tag{10}$$

where b_j is the thickness of layer j; $c_{v,j}$ is the consolidation coefficient of layer j; $\widetilde{c_v}$ is the equivalent consolidation coefficient of a cluster of consolidating layers; and n is the number of consolidating layers between drained layers. Here, it should be noted that a drained layer has a degree of consolidation equals to 100 %.

Using Eqs. 8 and 9 final compaction of each layer can be calculated by multiplying degree of consolidation of a layer at a specific time and its settlement at that time.

3 Case Study

The methodology described in this paper is applied to land subsidence calculation in northern Jakarta, Indonesia. The northern part of the Jakarta plain shows a significant amount of land subsidence. The upper few hundred meters of the subsurface in the area consist of relatively young highly deformable sediments (mainly Quaternary clays and silts). Since the 1980s, considerable regional declines of the deeper groundwater piezometric levels have occurred as a result of deep groundwater abstraction. In addition, remarkable urban development with many buildings and other heavy constructions has added external surcharge to the subsurface that have to be supported by the earth formations underneath. On different scales of time and space one thus would expect three different types of land subsidence that can be expected to occur in the Jakarta basin, namely: 1) subsidence due to groundwater extraction, 2) subsidence induced by the load of constructions, and 3) subsidence due to geotectonic factors. The expected rates for the latter are few order-of-magnitudes smaller than land subsidence due to groundwater abstraction at its early stages (i.e. during the period 1965-1989). In addition, there are clear evidences for land subsidence due to the load (surcharge) imposed by urban constructions at a number of locations in Jakarta; however, this

type of land subsidence tends to be rather local (Abidin et al. 2011). Meanwhile, the rather striking relationship between the patterns and distribution of piezometric drawdowns and of observed land subsidence supports the hypothesis that the main cause of the observed regional land subsidence in the Northern (coastal) area of Jakarta is the abstraction of deep groundwater.

3.1 Study Area

The province of Jakarta (or DKI Jakarta) is located on the northwest coast of the Java Island of Indonesia. DKI Jakarta occupies a total area of about 720 km^2 with about 32 km coast line. The province lies in a low flat basin (between -2 m and 50 m above mean sea level) creating a valley in the northern areas separated by comparatively hilly areas in the southern parts of the province. About 40 % of DKI Jakarta (particularly the northern areas) is below sea level (see Fig. 1). This, in fact, significantly contributes to the province's vulnerability
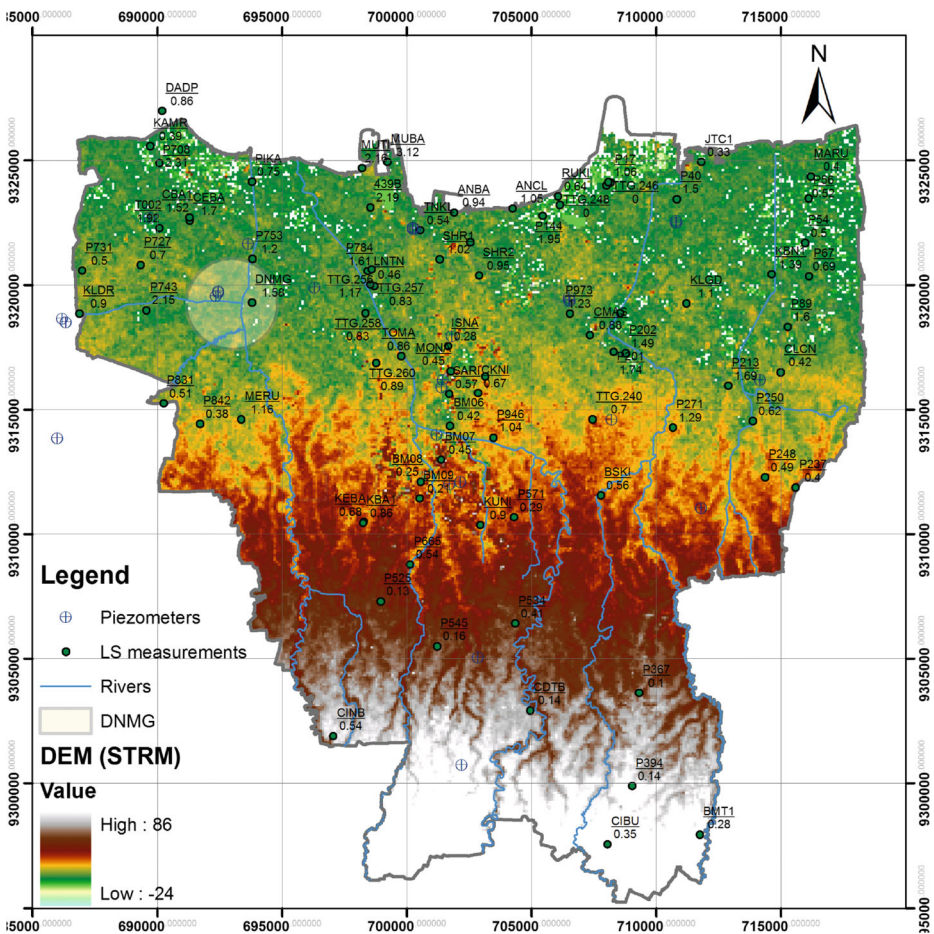

Fig. 1 Study area, Digital Elevation Model (DEM) using Shuttle Radar Topography Mission (SRTM) data, and selected location (DNMG) for analysis

to flood risks either by sea or rivers. In this paper, calculation is performed at the DNMG area (Fig. 1) where piezometric head and land subsidence data are partially available to demonstrate possible impacts of groundwater management on land subsidence using the methodology described here.

3.1.1 Lithological and Hydrogeological Description

The geological/hydrogeological reality of the study area (based on drilling data) is far too complex to be mapped precisely (IWACO et al. 1994a); it happens so often that an aquifer could be formed by a combination of small sand lenses that may be found at a certain depth range. The study area represents a coastal plain with a shallow aquifer that consists of marine clay underlain by volcanic fan depositions. This aquifer has no much potentiality for groundwater development since it has low permeability and/or it is highly vulnerable to contamination. In addition, the deeper aquifer zone consists of marine deposits with some sand lenses. This deeper aquifer zone is already overexploited and it imposes considerable risks for land subsidence. Borehole data show that clay and clayey sediments dominate the hundreds of meters thick basin fill of the lower coastal zone of Jakarta plain; however, it is far too difficult to correlate distinct sediment layers in terms of aquifer and aquitard formations (IWACO et al. 1994a). This is due to the relatively sparse and thin sand layers of relatively limited lateral extent encountered in the drilling data. Because of the many uncertainties in such geological setting, a rather synthetic lithological sequence is used in this study (see Fig. 2).
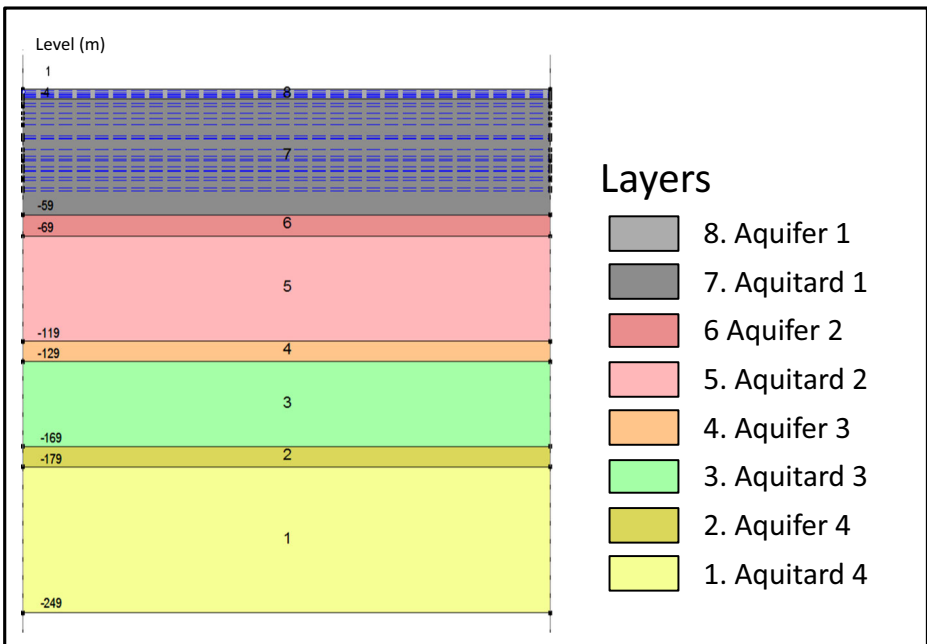

Fig. 2 Conceptual lithological sequence of aquifer/aquitard formations (lines in blue demonstrate piezometric heads used in this analysis)

3.1.2 Piezometric Head Data

IWACO et al. (1994b) discusses the spatial and temporal variability of the piezometric heads in the study area. It shows that the piezometric levels of deep groundwater are declining strongly in response to groundwater abstraction from deep wells. Till early 1970s, the deeper groundwater was still (to a great extend) artesian; nowadays the static water levels within the coastal zone are tens of meters below mean sea level. A strong decline in piezometric levels in the early 1970s was observed from available data for all deep layers. Groundwater piezometric head data in IWACO et al. (1994b) and Maathuis et al. (1996) are used in this paper to construct a conceptual hydrographs of the piezometric heads for the four aquifers considered here. Figure 3 shows piezometric head hydrographs of all considered scenarios. Piezometric heads in the period 1965-2005 (with 5 years long stress periods) are used to simulate and calibrate the developed land subsidence model. As discussed earlier, the calibration period of available data shows a general trend of declining piezometric heads in the three bottom aquifer layers. The figure shows that most of groundwater abstraction around the study area comes from aquifer 2 and aquifer 3. Here, it should be noted that stress period at 2005 is used to evaluate the land subsidence in 2010 which is the year of the last land subsidence measurement (see next section) used in model calibration of this study. The hydrographs after 2005 till 2030 show the adopted groundwater management scenarios of this study.

3.1.3 Land Subsidence Data

Since the early 1980s, several land subsidence measurement techniques (e.g. GPS surveys, and InSAR technique) have been applied to measure the land subsidence in Jakarta (Abidin et al. 2008). The results obtained from these measurements over the period between 1982 and 2010 show that land subsidence in Jakarta is spatially and temporally distributed. In general, it was found that the subsidence rates are about $1 - 15\ cm/year$; however, a few
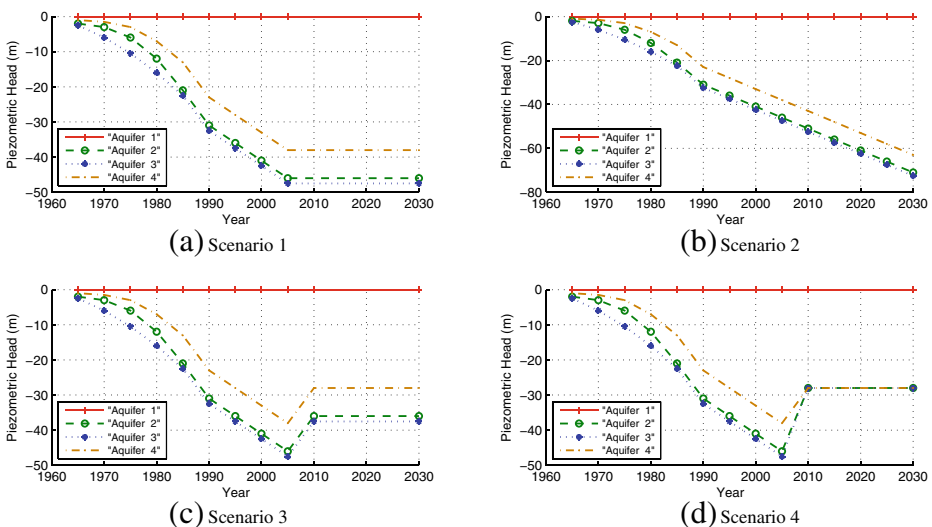

Fig. 3 Piezometric heads of the four considered scenarios

Table 1 Land subsidence data at DNMG location

Year	Time Step (day)	Subsidence (m)
1974	3285	0.28
1991	9490	0.48
1992.4	10000	0.55
1995	10950	0.68
2000	12775	0.83
2005	14600	1.24
2010	16425	1.64

locations can have the subsidence rates up to about $20 - 28\ cm/year$ (Abidin et al. 2011). A combined data set collected during the project "Jakarta Coastal Defence Strategy", Deltares et al. (2011), is used in the analysis performed here. Measured values of land subsidence at the DNMG location (see Fig. 1) are given in Table 1. These values are used to condition the land subsidence models parameters of the NEN-Bjerrum method using the Maximum a Posteriori method.

3.2 Land Subsidence Model Calibration

The land subsidence model developed here uses the lithological profile shown in Fig. 2, and piezometric head time series in the period 1965-2005 as shown in Fig. 3. The latter is used to calculate changes of pore water pressure over time and hence to calculate effective stresses according to Eq. 1. To be able to forecast response of the developed model to groundwater management scenarios, the model is conditioned on available land subsidence measurements (see Table 1). For this purpose, the Maximum a Posteriori (MAP) formulation is adopted. The method solves a special Weighted Least Squares (WLS) problem by minimizing not only the difference between measurements and predictions, but also the difference between initial values and the updated values of the geo-mechanical parameters to be estimated. The optimum solution of this problem is a compromise between these two terms. Table 2 shows values of the geo-mechanical parameters of the selected solution. Four different parameters are estimated for each aquitard layer; namely: compression ratio (CR), re-compression ratio (RR), secondary compression index (C_α), over consolidation ratio (OCR), and consolidation coefficient (c_v). Here, it should be noted that the over consolidation ratio is a surrogate function of the pre-consolidation pressure (σ_p). It

Table 2 Values of calibrated geo-mechanics parameters

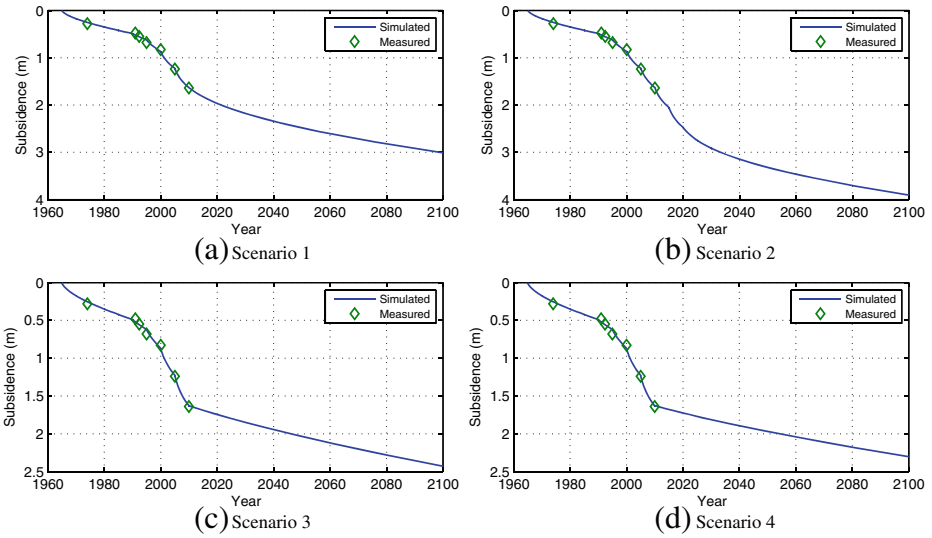| Layer	$RR\ [-]$	$CR\ [-]$	$C_\alpha\ [-]$	$OCR\ [-]$	$C_v\ [m^2/s]$
Aquitard 1	0.001	0.600	0.013	1.52	9.38E-07
Aquitard 2	0.002	0.044	0.030	1.27	4.31E-09
Aquitard 3	0.004	0.285	0.009	5.05	1.39E-08
Aquitard 4	0.048	0.225	0.005	4.06	2.52E-09

Fig. 4 Calculated versus measured subsidence and forecasted subsidence for the four considered scenarios

is defined as the ratio between the pre-consolidation pressure and the initial vertical effective soil pressure. Table 2 shows large over-consolidation ratios (OCR) of the two bottom aquitard layers indicating older age and/or higher stresses experienced over time. Figure 4 shows simulated versus measured land subsidence at the study area. As the figure shows, a very good agreement among simulated and measured land subsidence is obtained using the calibrated parameter values. Furthermore, Fig. 5 shows compaction of each layer which indicates their contributions to total land subsidence. The figure shows that total land subsidence is obtained basically by compaction of the most top and following aquitard layers (i.e. "Aquitard 1" and "Aquitard 2"). To examine consolidation more closely, Fig. 6 shows degree of consolidation, see Eq. 9, of the four aquitard layers. Delay effects due to slow pore
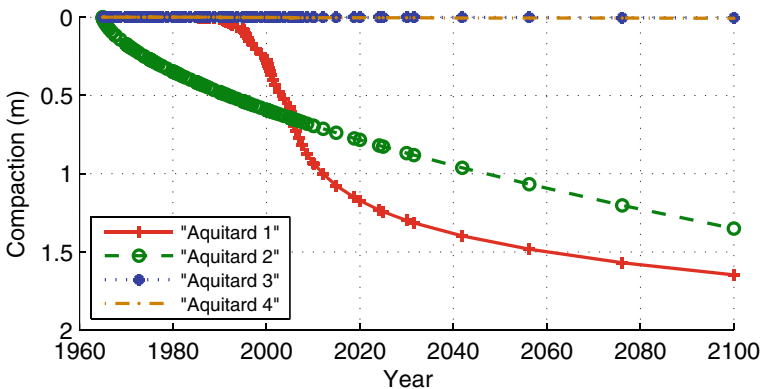

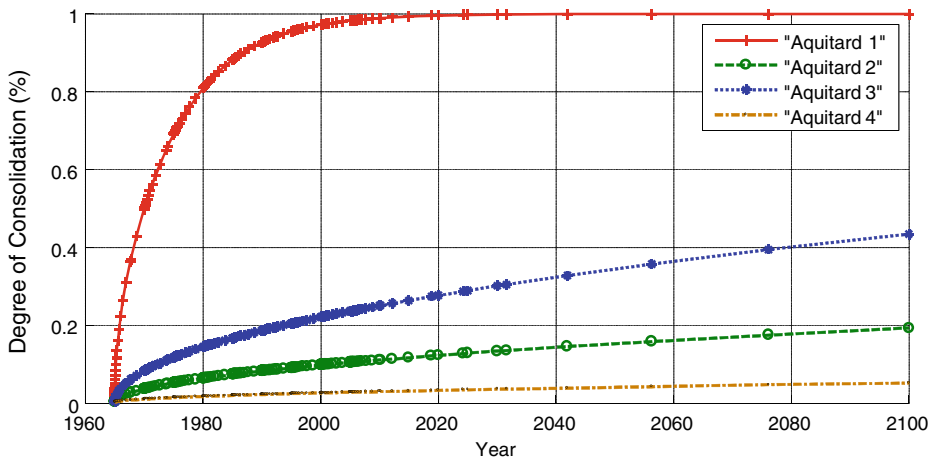**Fig. 5** Compaction of aquitard layers (Scenario 1)

Fig. 6 Degree of consolidation of aquitard layers

water dissipation can be noticed for all aquitards especially for the most bottom one. This is basically because of the assumption that the lower boundary of the most bottom aquitard is impervious (hence, it is un-drained). The un-drained lower boundary can be simply justified because the layer is assumed to be overlaid on basement rocks. Also, thickness of aquitard layers plays important role on degree and required time for total dissipation of excess pore water pressure. The figure also shows that "Aquitard 2", which contributes significantly to total subsidence, reaches only 20 % of total consolidation by 2100. This is due to slow dissipation of excess pore water pressure as a result of small consolidation coefficient (see Table 2).

3.3 Effects of Groundwater Management on Land Subsidence

In this section, we examine effects of different plausible groundwater management scenarios on predicted land subsidence in northern Jakarta. Four different scenarios are considered to forecast land subsidence between years 2010 and 2100. They are namely 1) "Scenario 1": drawdown for all aquifers are kept zero till 2100 by maintaining piezometric levels at their values of 2010; 2) "Scenario 2": drawdown for all aquifers increase 5 *m* every 5 years from 2010 till 2030; 3) "Scenario 3": piezometric heads are recovered for all aquifers by 2015 to their values of 1995, 4) "Scenario 4": piezometric heads are recovered for all aquifers by 2015 to the maximum level of all aquifers in 1995. Figure 3 shows piezometric heads hydrographs for the four examined scenarios (between 2010-2030)

Table 3 gives the forecasted land subsidence at years 2020, 2025, 2030, and 2100 for all scenarios. Maintaining piezometric heads for all aquifers at the levels of 2010 (i.e., Scenario 1) has not stopped ground surface to settle. Even though the last water load applied for "Scenario 1" is in 2010, land subsidence continues over time to reach 3.01*m* by 2100. This means that a residual subsidence of 1.37*m* between 2010 and 2100 is expected. This can be explained by both delayed pore water pressure dissipation and visco-plastic creep compaction. This means that even if effective stresses along the profile do not change after 2010, land subsidence will continue till all layers reach hydrostatic equilibrium and creep compaction of all layers vanish by time due to aging.

As may be expected, applying further drawdowns leads to more land subsidence as indicated by the results of scenario "2" which is a more plausible scenario for groundwater usages and demands. Table 3 shows that scenario "2" (i.e., increasing drawdown at a rate of 1 $m/year$ from 2010 till 2030 with a 5-year time step) leads to a higher predicted land subsidence than scenario "1". The table shows that land subsidence is estimated as 2.18m for year 2030 using scenario "1", while it is estimated as 2.92m for the same year using scenario "2". This means that in 2030 an increase of 0.74m in land subsidence is expected if scenario "2" is adopted instead of scenario "1". Values obtained from the two scenarios deviate even more for the 2100 land subsidence estimation where it is estimated as 3.91m for scenario "2" with an increase of 0.90m from the value estimated for scenario "1" (3.01m). To examine effects of piezometric heads recovery on predicted land subsidence, scenarios "3" and "4" are considered. Aquifers piezometric heads recovery can be achieved by stopping pumping while aquifers are replenished by fluxes from boundaries, natural recharge; or artificial recharge. Scenario "3" assumes piezometric heads recovery to the levels of 1995 for each aquifer, while scenario "4" assumes piezometric heads recovery to $-28m$ for all aquifers which is the maximum level of heads in aquifer 2, aquifer 3, and aquifer 4 in year 1995 (i.e., the maximum of $-36m$, $-37.5m$, $-28m$); see Fig. 3. Both scenarios assume application of these recoveries by 2015. Although piezometric heads recovery will decrease effective stresses along the subsurface profile, land subsidence for both scenarios are estimated to continue; however, at lower rates than those estimated for scenarios "1" and "2". Meanwhile, scenario "3" estimates land subsidence in 2100 as 2.43m with a reduction of 0.59m than the value calculated for scenario "1". The reduction depicted in the calculated land subsidence for scenario "4" is even more at a value of 0.71m from the one calculated using scenario "1".

Contribution of the creep component to the total land subsidence is investigated by setting the coefficient of secondary compaction (C_α) of all layers to zero for scenario "1". A total land subsidence of 0.024m for the year 2100 is obtained indicating a significant contribution of the creep compaction to the total land subsidence as compared to the reference scenario "1" (i.e. 3.01m) for the parameters set considered here. We further examine effects of several combinations of "No Creep" and "Drained" conditions on calculated land subsidence using scenario "1" as a reference case. A drained layer achieves a hydrostatic condition immediately after changing pore water pressure within or along boundaries of the layer; this means that degree of consolidation is 100% since beginning of the simulation. Four of such combinations are examined here; they are, namely, 1) "CrNoDr" which is the case for creep and no-drained condition (this is scenario "1"); 2) "CrDr" which is the case for creep and drained condition; 3) "NoCrNoDr" which is the case for no-creep and no-drained condition; and 4) "NoCrDr" which is the case for no-creep and drained condition. Fig. 7 shows land subsidence of these four cases. Influence of the creep component explained before is based on "CrNoDr" and "NoCrNoDr" cases. Similar conclusion about

Table 3 Forecasted land subsidence (m) for the considered scenarios

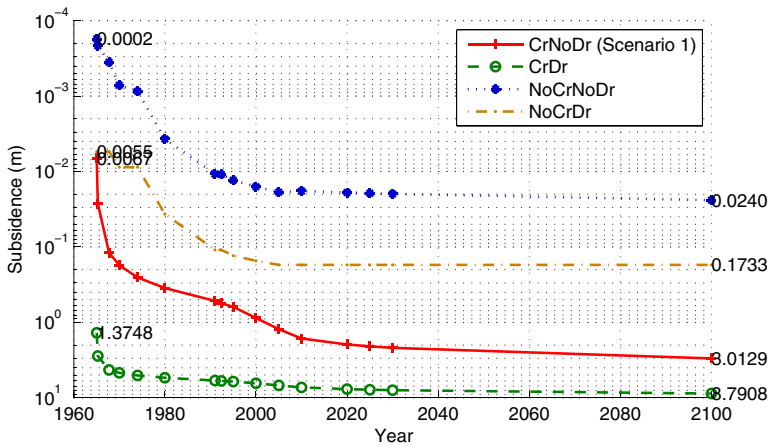| Year	Scenario 1	Scenario 2	Scenario 3	Scenario 4
2020	1.97	2.48	1.74	1.73
2025	2.08	2.75	1.80	1.77
2030	2.18	2.92	1.85	1.81
2100	3.01	3.91	2.43	2.30

Fig. 7 Subsidence for several drainage and creep conditions of scenario "1"

significant contribution of the creep compaction to total land subsidence can be obtained by comparing "CrDr" and "NoCrDr" cases. Moreover, comparing "CrNoDr" and "CrDr" cases show impacts of the consolidation process on calculation of the total land subsidence. The earlier calculates subsidence in 2100 as $3.01m$ while the latter calculates it as $8.79m$. This means that only 34% of expected land subsidence under drained condition takes place in 2100 due to the consolidation process. This, in fact, means that the coupled processes of creep and consolidation leads to a favorable situation where the consolidation process causes a reduction of expected land subsidence under fully drained conditions. This is especially the case for early times which are characterized by higher rates of land subsidence.

4 Conclusions and Recommendations

The NEN-Bjerrum method has been used to evaluate land subsidence in deltaic environment due to change in pore water pressures as a result of applying different groundwater management schemes. The method is combined with the Terzaghis consolidation theory to account for consolidation of multiple homogeneous layers of soil between drained layers. The method decomposes total strain into a direct elastic contribution (ε_d) and a transient visco-plastic contribution (ε_{vp}). For the case study considered here, the year 1965 is considered as the reference year with no land subsidence due to very limited groundwater abstraction. The model has been calibrated on land subsidence data available within the period 1974-2010 using a MAP formulation, and has produced good agreement between measured and simulated land subsidence values. The model is then used to forecast land subsidence for years 2020, 2025, 2030 and 2100. Effects of four groundwater management scenarios have been evaluated using the developed calibrated model. For the reference scenario ("1"), in which piezometric levels of all aquifers were maintained at their values of 2010, the model forecasted $1.38m$ of residual land subsidence between 2010-2100. Meanwhile, the most plausible groundwater management scenario (i.e. scenario "2") of continues drawdown till 2030 has produced a larger residual land subsidence ($2.27m$) for the same period. However, for the extreme piezometric levels recovery case (scenario "4"), in which

piezometric levels of all aquifers were recovered by 2015 to the maximum piezometric level of all aquifers in 1995, the model estimated 0.68m of residual land subsidence between 2010-2100. Hence, it was observed that the land subsidence would continue for all examined scenarios, however, at different rates. The percentage between residual land subsidence between 2010 and 2100 and land subsidence of 2010 (i.e. 1.64m) were estimated as 84 %, 139%, 49 %, and 41 % for the four examined scenarios, respectively.

This study also highlighted effects of creep compaction and soil consolidation on calculated total land subsidence. Different combinations of considering creep and consolidation were examined. The results showed significance of creep compaction on calculated land subsidence where for the case studied here with the calibrated parameters set, creep presented about 99 % of total land subsidence for the year 2100. The results also showed that coupled processes of consolidation and creep produced a favorable situation where consolidation reduced total land subsidence by 66 % as compared to the case of drained layers (and consequently 100 % consolidation).

The damage that may be caused by land subsidence may have several folds. Wherever land subsidence occurs, damage to infra-structures (e.g. pipelines) may be produced. However, the impacts of flooding and drainage probably will be more critical since it will be more spatially distributed. Land subsidence in low-lying coastal zones is expected to bring part of the land under mean sea level. This will reduce in return topographic gradients needed for adequate drainage, and consequently, risks to floods will be increased. This will be even manifested by climate changes and sea level rise. An integrated approach is recommended to address such multi-disciplinary problem. This includes the development of a coupled groundwater flow and subsurface deformation that accounts for secondary compaction and spatial variability of the problem. Such coupled system of groundwater flow and land subsidence models should also be integrated within a flood risk management system (including flood inundation capabilities) to manage risks due to land subsidence as related to groundwater and flood management.

References

Abidin HZ, Andreas H, Djaja R, Darmawa D, Gamal MJ (2008) Land subsidence characteristics of jakarta between 1997 and 2005, as estimated using gps surveys. GPS Solutions 12(92):23–32

Abidin HZ, Andreas H, Gumilar I, Fukuda Y, Deguchi T (2011) Land subsidence of Jakarta (Indonesia) and its relation with urban development. Nat Hazards 59:1753–1771. doi:10.1007/s11069-011-9866-9

Bjerrum L Engineering geology of norwegian normally consolidated marine clays as related to settlements of buildings. Geótechnique 17(2):81–118

Borja RI, Kavaznjian E (1985) A constitutive model for the σ-ϵ-t behaviour of wet clay. Géotechnique 35:283–298

Buisman K (1936) Results of long duration settlement tests. In: Proceeding 1st International Conference on Soil Mechanics and Foundation Engineering, Massachusetts, 1: Cambridge, Massachusetts, 1, Cambridge, pp 103–106

Burkett VR, Zilkoski DB, Hart DA (2002) Sea-level rise and subsidence: Implications for flooding in new orleans louisiana. In: US Geological Survey Subsidence Interest Group Conference, US Geological Survey, Galveston, TexasUS, Geological Survey, Galveston, Texas, pp 3–71

Calderhead AI, Martel R, Garfias J, Rivera A, Therrien R (2012) Water Resour Manag 29:1847–1864

Deltares, Urban Solutions, Witteveen + Bos, Triple-A Team, MLD, Pusair, Bandung Institute of Technology (2011) Jakarta coastal defence atlas. Project: Jakarta coastal defence strategy, Deltares

Den Haan EJ (1994) Vertical compression of soils. PhD thesis, Technical University of Delft

Ericson JP, Vörösmarty CJ, Dingman SL, Ward LG, Meybeck M (2006) Effective sea-level rise and deltas: Causes of change and human dimension implications. Global Planet Chang 50:63–82

Galloway DL, Burbey TJ (2011) Review: Regional land subsidence accompanying groundwater extraction. Hydrogeol J 19(8):1459–1486

Garlanger JE (1972) The consolidation of soils exhibiting creep under constant effective stress. Geotechnique 22(1):71–78

Green TR, Taniguchi M, Kooi H, Gurdak JJ, Allen DM, Hiscock KM, Treidel H, Aureli A (2011) Beneath the surface of global change: Impacts of climate change on groundwater. J Hydrol 405(3-4):532–560. doi:10.1016/j.jhydrol.2011.05.002

Gu C, Hua L, Zhang X, Wang X, Guo J (2011) Climate change and urbanization in the yangtze river delta. Habitat Int 35:544–552

Helm DC (1975) One-dimensional simulation of aquifer system compaction near pixley, California, (1) constant parameters. Water Resour Res 11:198–112

Helm DC (1976) One-dimensional simulation of aquifer system compaction near pixley, California, (2) stress-dependent parameters. Water Resour Res 12:375–391

Holzer TL (1981) Preconsolidation stress of aquifer systems in areas of induced land subsidence. Water Resour Res 17:693–704

Huang B, Shu L (2012) Groundwater overexploitation causing land subsidence: Hazard risk assessment using field observation and spatial modelling. Water Resour Manag 26:4225–4239

IWACO, Delft Hydaulics, TNO (1994a) Jabotabek water resources management study, volume 6. Tech. rep. Ministry of Water Resources

IWACO, Delft Hydaulics, TNO (1994b) Jabotabek water resources management study. volume 7, Tech. rep. Ministry of Water Resources

Jacob CE (1940) On the flow of water in an elastic artesian aquifer. Am Geophys Union Trans 2:574–586

Leake SA, Galloway DL (2007) MODFLOW ground-water model, User guide to the Subsidence and Aquifer-System Compaction Package (SUB-WT) for Water-Table Aquifers: U, Techniques and Methods, vol Book 6. U.S. Geological Survey

Maathuis H, Yong RN, Adi S, Prawiradisastra S (1996) Development of groundwater management strategies in the coastal region of Jakarta, Indonesia: final report. Tech. rep., Saskatchewan Research Council, Saskatoon, SK, CA

MATLAB (2011) version 7.13.0 (R2011). The MathWorks Inc. Natick, Massachusetts

Meinzer OE (1928) Compressibility and elasticity of artesian aquifers. Econ Geol 23(3):263–291

Mesri G, Vardhanabhuti B (2005) Secondary compression. J Geotech Geoenviron Eng ASCE 131:398–401. doi:10.1061/(ASCE)1090-0241(2005)131:3(398)

NNI (1991) Geotechnics - Calculation Method for shallow foundations (in Dutch). Nederlands Normalisatie Instituut (Dutch Normalization Institute), pp 31

Onta PR, Gupta AD (1995) Regional management modelling of a complex groundwater system for land subsidence control. Water Resour Manag 9:1–25

Tang JCS, Vongvisessomjai S, Sahasakmontri K (1992) Water Resour Manag 6:47–56

Taylor D (1942) Research on consolidation of clays In: Series 82. Massachusetts Institute of Technolology, Cambridge, Massachusetts

Terzaghi K (1925) Settlement and consolidation of clay. McGraw-Hill, New York, pp 874–878

Theis CV (1935) The relation between the lowering of the piezometric surface and the rate and duration of discharge of a well using groundwater storage. Am Geophys Union Trans 16:519–524

Tóth J (1995) Hydraulic continuity in large sedimentary basins. Hydrogeo J 3(4):4–16

Vermeer PA, Neher HP, Vogler U, Bonnier PG (2002) 3d creep analysis of the leaning tower of pisa tech. rep. Technical report. Kroener, Stuttgart University, p 48

Wilson AM, Gorelick S (1996) The effects of pulsed pumping on land subsidence in the santa clara valley, California. J Hydrol 174:375–396

Zhang Y, Xuea YQ, Wua JC, Yea SJ, Weib ZX, Lib QF, Yuc J (2007) Characteristics of aquifer system deformation in the southern yangtse delta, China. Eng Geol 90(3-4):160–173